VERSITA

Acta Geophysica
vol. 62, no. 3, June 2014, pp. 451-468
DOI: 10.2478/s11600-013-0173-6

Geodetic Constraints on the Period of Episodic Tremors and Slips Using Least Squares Harmonic Estimation Method with Application to Cascadia Subduction Zone

Roya MOUSAVIAN and Masoud M. HOSSAINALI

Department of Geodesy and Geomatics Engineering,
K.N. Toosi University of Technology, Tehran, Iran
e-mails: R_mousavian@yahoo.com, Hossainali@kntu.ac.ir

Abstract

It is expected that episodic tremors and slips (ETS) as a type of slow earthquakes with periodic property will be detected using harmonic estimation techniques. The principal goal of this paper is the detection of these kinds of earthquakes using least squares harmonic estimation (LS-HE). To accomplish this, the raw time series of 38 permanent GPS stations of the Pacific Northwest Geodetic Array have been analyzed. Previously, some independent techniques could confirm the occurrences of the aforementioned quakes at these stations. However, the current research intends to evaluate the spectrum of each of the de-trended time series using the LS-HE method. In each station, the period of the detected harmonic with the maximum power spectrum is equivalent to the average period previously reported for these events. According to the obtained results, the recurrence interval of these events ranges from 9 months to 3 years. In sum, the study confirms this method being efficient for investigating the occurrences of ETSs when the length of the GPS time series is sufficiently large.

Key words: episodic tremors and slips, slow earthquakes, least squares harmonic estimation, GPS.

1. INTRODUCTION

Slow earthquakes refer to a group of seismic events which includes: low frequency earthquakes (LFEs) (Obara *et al.* 2005), non-volcanic tremors (Obara 2002), slow slip events (SSEs) (Linde *et al.* 1996), episodic tremors and slips (ETSs) (Rogers and Dragert 2003, Miller *et al.* 2002, Julian 2002) and very low frequency earthquakes (VLFs) (Ito and Obara 2006).

Deep non-volcanic tremor (NVT) is a weak but persistent shaking phenomenon of the earth that was first observed in Japan's Nankai trough subduction zone (Obara 2002). The seismic records of these events are continuous noise-like waveforms. It means that signals are not impulsive like those of regular earthquakes; hence, routine methods cannot be applied for detecting the location of their positions' origins. Contrary to regular earthquakes which are impulsive and quick (usually complete in a few seconds), the deep non-volcanic tremors, at each occurrence, vibrate the earth for hours, days, or even for weeks. These events are most prominent in the 1-10-Hz frequency band (Beroza and Ide 2011). Non-volcanic tremors are simply referred to as tremors or tectonic tremors, which are episodic in nature and their loci slowly migrate along-strike at the speed of approximately 10 km per day (Beroza and Ide 2011).

Like regular ones, slow earthquakes are accompanied with fault slips, but since their duration is much longer, they are called slow earthquakes. The behavior of slow slip events (SSE) as a kind of slow earthquakes is very periodic and they are different from irregular behavior of the ordinary earthquakes.

Both slow slip and deep tremors occur along the subduction zones periodically where the seismic activity ranges from several days to several weeks, with the occurrence depth ranging between 30 and 40 km. Since the two phenomena occur simultaneously, the absence of one is an indication of the lack of the other (Beroza and Ide 2011). As seismic records provide the first evidences to the problem, their analysis tends to establish temporal and spatial correlations between the two phenomena which are called as the episodic tremor and slip (ETS).

ETS is the name of a plate boundary phenomenon recently discovered in northern Cascadia (see Rogers and Dragert 2003). ETSs are repeated and transient ground motions at plate margins that occur opposite to the direction of longer-term inter-seismic deformation and are accompanied by low-frequency, emergent and semi-continuous seismic signals. Because of the three essential components of these events, that is: transient ground motions, tremor-like seismic signals, and episodic occurrences, extraction of the corresponding long term periodicities in detailed ETS studies requires continu-

ous seismic and geodetic observations from a dense network over a long period of time.

The seismological phenomenon ETS consists of tremors and slips. In order to investigate the tremors, one must focus on seismic data; however, the evaluation of slips requires geodetic measurements (e.g., Rogers and Dragert 2003, Kao *et al.* 2005, 2009, Ito *et al.* 2007, Szeliga *et al.* 2008, Holtkamp and Brudzinski 2010).

Generally, to identify the approximate temporal and spatial distribution of the aforementioned seismic events, two methods: Source-Scanning Algoritm (Kao and Shan 2004) and Tremor Activity Monitoring System (TAMS) (Kao *et al.* 2007, 2008), are frequently applied. However, various other methods have also been developed for identifying approximate slips. Rogers and Dragert (2003) identified the approximate dates for slip transients by applying a sawtooth function that was correlated with the detrended coordinate time series. They established the maximum for cross-correlation function as the midpoint of slip events. Szeliga *et al.* (2008) applied wavelet transformation for detecting the onset time of ETSs in the geodetic time series of some stations located throughout the long dipping fault of Cascadia subduction zone. They have also estimated recurrence range for the occurrence of the seismic events in northern, middle, and southern parts of Cascadia. Haltkamp and Brudzinski (2010) used a hyperbolic tangent curve fitting technique for identifying the duration of slow slips and displacement magnitudes using GPS time series along the margin of Cascadia, independent of seismic tremor records.

The current paper discusses the application of LS-HE method in detecting the mean period of the slow slip events. This method was first introduced and applied to GPS position time series by Amiri-Simkooei (see Amiri-Simkooei 2007, Amiri-Simkooei *et al.* 2007). Principals of this method will be introduced in the next section of this paper. Since the periods of these events in Cascadia are known, working on this area can help provide an appropriate criterion for evaluating the efficiency of the LS-HE method as an automatic technique. The method has been applied to 38 GPS stations located in the Cascadia subduction zone. The last section discusses on the obtained numerical results.

2. LEAST SQUARES HARMONIC ESTIMATION (LS-HE)

Least squares harmonic estimation (LS-HE) is based on the application of harmonic functions for modeling the periodic constituents of a time series. As a generalization of the Fourier spectral analysis, LS-HE is neither limited to evenly spaced data nor to integer frequencies (Amiri-Simkooei and Asgari 2012). The method is actually based on the least squares spectral analysis

(LSSA) developed by Vaníček when an initial design matrix is present in the model and the covariance matrix, in general, is not a scaled identity matrix (Vaníček 1996). Amiri-Simkooei and Tiberius (2007) and Amiri-Simkooei and Asgari (2012) have provided some examples for the application of this method. Mousavian and Hossainali (2012) also investigated the method's efficiency for detecting frequencies in a simulated time series as well as the main tidal constituents. The results from simulated time series suggest that the LS-HE method is sensitive to the amplitudes of the existing components. This is seen through the rejection of those constituents whose amplitudes are smaller than the others by the statistical test of this method. Nevertheless, increasing the length of a time series increases the reliability of the obtained results. This is seen through the detection of new harmonic constituents in both of simulated coordinates and tidal time series by increasing the length of the corresponding records.

This paper is the first attempt to apply the LS-HE method for the detection of slow earthquakes.

The functional model of a periodic time series $\mathbf{y}^T = [y_1, y_2, \ldots, y_m]$, which is defined on R^m, is given as:

$$\mathbf{y} = \mathbf{y}_0 + r\mathbf{t} + \sum_{k=1}^{q} a_k \cos(\omega_k \mathbf{t}) + b_k \sin(\omega_k \mathbf{t}) \tag{1a}$$

or in the matrix notation:

$$\mathbf{y} = \mathbf{A}\mathbf{x} + \sum_{k=1}^{q} \mathbf{A}_k \mathbf{x}_k \ . \tag{1b}$$

In these equations, $\mathbf{y}_0$ is the zero frequency component of the time series, r is the linear rate, a_k and b_k are the amplitudes of sine and cosine components corresponding to the frequency ω_k and t_i for $i = 1, 2, ..., m$ are the observation epochs. The two column matrix $\mathbf{A}$ contains the coefficients of the linear regression part of the model whereas the two column matrices $\mathbf{A}_k$ are constructed by the corresponding coefficients for the trigonometric components of frequencies ω_k:

$$\mathbf{A}_k = \begin{bmatrix} \cos\omega_k t_1 & \sin\omega_k t_1 \\ \cos\omega_k t_2 & \sin\omega_k t_2 \\ \vdots & \vdots \\ \cos\omega_k t_m & \sin\omega_k t_m \end{bmatrix}, \quad \mathbf{x} = \begin{bmatrix} y_0 \\ r \end{bmatrix}, \quad \mathbf{x}_k = \begin{bmatrix} a_k \\ b_k \end{bmatrix}. \tag{2}$$

The LS-HE method has been proposed for finding the unknown parameters in Eq. 1 when the unknown parameters are both ω_k and the coefficients a_k and b_k. For that matter, first the unknown frequencies $\omega_1, \omega_2, \ldots, \omega_q$ are

determined. This is done recursively through the following q statistical hypotheses in which i runs from 1 to q (Amiri-Simkooei 2007):

$$\begin{cases} H_0: \ \mathbf{y} = \mathbf{A}\mathbf{x} + \sum_{k=1}^{i-1} \mathbf{A}_k \mathbf{x}_k \\ H_a: \ \mathbf{y} = \mathbf{A}\mathbf{x} + \sum_{k=1}^{i} \mathbf{A}_k \mathbf{x}_k \end{cases} . \tag{3}$$

Accepting the null hypothesis at each run adds a new frequency (component) to the proposed functional model. Evaluation of this hypothesis test consists of the two steps (Amiri-Simkooei 2007):

(i) solving the following maximization problem in order to detect the existing frequency ω_i (Amiri-Simkooei 2007, Teunissen 2000):

$$\omega_i = \arg\max_{\omega_j} \left\| \mathbf{P}_{\bar{\mathbf{A}}_j} \mathbf{y} \right\|^2_{\mathbf{Q}_y^{-1}}, \qquad \bar{\mathbf{A}}_j = \mathbf{P}^{\perp}_{\bar{\mathbf{A}}} \mathbf{A}_j \ , \tag{4a}$$

$$\mathbf{P}^{\perp}_{\bar{\mathbf{A}}} = \mathbf{I} - \bar{\mathbf{A}} \left(\bar{\mathbf{A}}^T \mathbf{Q}_y^{-1} \bar{\mathbf{A}} \right)^{-1} \bar{\mathbf{A}}^T \mathbf{Q}_y^{-1} \ , \tag{4b}$$

$$\mathbf{P}_{\bar{\mathbf{A}}_j} = \bar{\mathbf{A}}_j \left(\bar{\mathbf{A}}_j^T \mathbf{Q}_y^{-1} \bar{\mathbf{A}}_j \right)^{-1} \bar{\mathbf{A}}_j^T \mathbf{Q}_y^{-1} \ , \tag{4c}$$

where the operator $\|.\|^2_{\mathbf{Q}_y^{-1}}$ is the L2-norm, $\bar{\mathbf{A}} = \left[\mathbf{A}, \mathbf{A}_1, ..., \mathbf{A}_{i\text{-}1} \right]$, and $\mathbf{Q}_y$ is the variance-covariance matrix of observations. Sub-matrices $\mathbf{A}_i$ of matrix $\bar{\mathbf{A}}$ have the same structure as $\mathbf{A}_k$ given in Eq. 1 and are constructed using the frequencies which were detected through previous evaluations of the statistical hypothesis 3. The matrix $\mathbf{A}_j$ has the same structure as $\mathbf{A}_k$ and is constructed using the frequency of interest.

Since analytical solution of the optimization problem given in Eq. 4 is complicated, numerical methods are preferred to solve it. For this, the power spectrum of the time series is produced applying the spectral values of different frequencies ω_j which are computed by $\left\| \mathbf{P}_{\bar{\mathbf{A}}_j} \mathbf{y} \right\|^2_{\mathbf{Q}_y^{-1}}$. The continuous diagram in which the spectral values are plotted against their corresponding frequencies constructs the power spectrum of the time series. Consecutive frequencies with maximal spectral values are used to construct the matrices $\mathbf{A}_i$.

(ii) The hypothesis test 3 is then evaluated using $\mathbf{Q}_y = \sigma^2 \mathbf{I}$ in which the *a priori* variance of unit weight σ^2 is unknown. The following statistics is used for this purpose (see Teunissen *et al.* 2005, Amiri-Simkooei 2007):

$$T_2 = \frac{\left\| \mathbf{P}_{\bar{\mathbf{A}}_i} \mathbf{y} \right\|^2_{\mathbf{Q}_y^{-1}}}{2\hat{\sigma}_a^2} = \frac{\hat{\mathbf{e}}_0^T \mathbf{A}_i (\mathbf{A}_i^T \mathbf{P}_{\bar{\mathbf{A}}}^{\perp} \mathbf{A}_i)^{-1} \mathbf{A}_i^T \hat{\mathbf{e}}_0}{2\hat{\sigma}_a^2} \ . \tag{5}$$

In Eq. 5, $\bar{\mathbf{A}}_i = \mathbf{P}_{\bar{\mathbf{A}}}^{\perp} \mathbf{A}_i$, $\hat{\mathbf{e}}_0$ is the least squares residual under the null hypothesis and $\hat{\sigma}_a^2$ is *a posteriori* variance under alternative hypothesis, which is computed as follows:

$$\hat{\sigma}_a^2 = \frac{\hat{\mathbf{e}}_a^T Q_y^{-1} \hat{\mathbf{e}}_a}{df} \ , \tag{6}$$

where *df* and $\hat{\mathbf{e}}_a$ are the degree of freedom and the least squares residuals under the alternative hypothesis of the statistical test 5, respectively. The distribution of the statistics 5 is central Fisher (F-distribution) with 2 and $m - n - 2i$ degrees of freedom, that is:

$$T_2 \approx \mathbf{F}(2, m - n - 2i) \ . \tag{7}$$

At the next step, the remaining unknown parameters of the functional model, including the zero frequency component $\mathbf{y}_0$, linear rate *r* and amplitudes of the detected frequencies, are determined in the LS-HE method. According to the least squares method, the unknown parameters in the functional model given in Eq. 8 and the corresponding covariance matrix of these parameters are computed from the following equations:

$$\mathbf{y} = \mathbf{B}\mathbf{x} + \mathbf{v} \ , \tag{8}$$

$$\hat{\mathbf{x}} = \left(\mathbf{B}^T \mathbf{Q}_y^{-1} \mathbf{B} \right)^{-1} \mathbf{B}^T \mathbf{Q}_y^{-1} \mathbf{y} \ , \tag{9a}$$

$$\mathbf{Q}_{\hat{x}} = \left(\mathbf{B}^T \mathbf{Q}_y^{-1} \mathbf{B} \right)^{-1} . \tag{9b}$$

The design matrix **B** includes matrices **A** and $\mathbf{A}_k$, $k = 1, \ldots, j$, and **v** is the vector of random errors.

3. THE AREA OF STUDY AND NUMERICAL RESULTS

In this study, for detecting the episodic tremors and slips, the GPS time series of 38 permanent stations in the Pacific Northwest Geodetic Array (PANGA) located in Cascadia subduction zone have been used. Time series of the permanent GPS stations of this network is available for free through the webpage http://www.geodesy.cwu.edu/. The main criterion in selecting the stations has been the possibility of comparing the obtained results with

previous studies on the occurrence of these events. For this purpose, the time series of these stations have been investigated from 1996 to 2011.

The Cascadia subduction zone is located in the northwestern part of the United States and the southwestern part of Canada. The main rupture in this zone is a 1000 km long thrust fault extending from northern California to Vancouver Island. In this region, the Juan de Fuca plate is subducting beneath the North American plate. This interface is seismically active, and repeatedly ruptures every several hundred years with thrust earthquakes with magnitude of $M_w \sim 9$ (Atwater 1987, Satake *et al.* 1996, Aguiar 2007). Figure 1 illustrates the tectonic setting of this area.

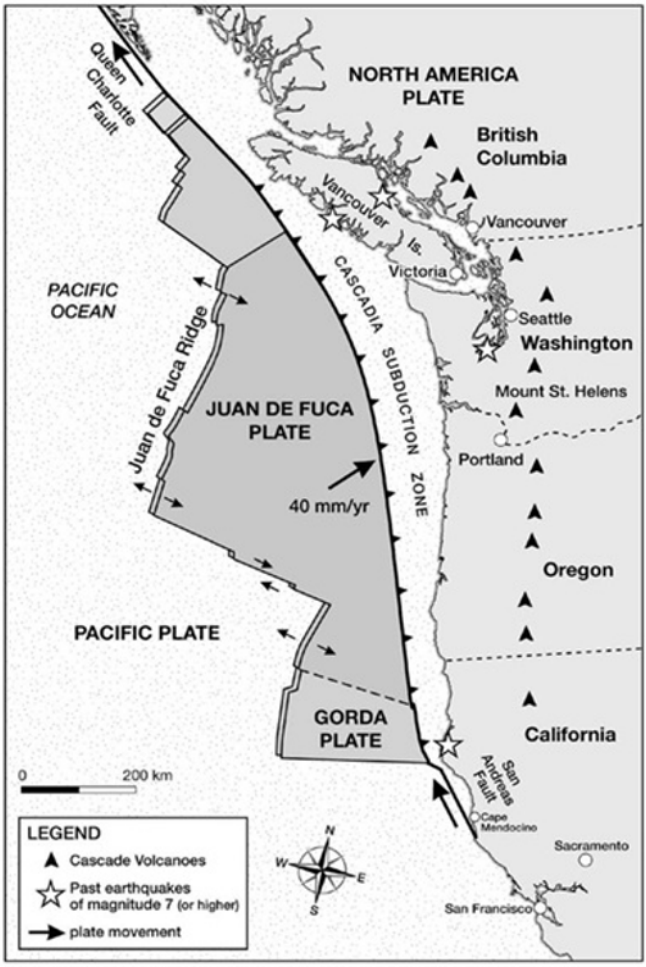

Fig. 1. The tectonic setting in the Cascadia subduction zone from Thompson (2011).

PANGA is a network of GPS receivers distributed throughout the northwestern part of the Pacific Ocean in the United States of America and Canada. This network monitors the crustal deformation using both the daily positioning of each station and measuring its movement relative to the other stations on the stable North American plate. The precise point positioning method is used to analyze the code and phase data of this network. For this purpose, using precise orbits, the position of the measuring station along with the other unknown parameters, such as receiver clock error, is calculated by GIPSY/OASIS II software (Miller *et al.* 2002, Szeliga *et al.* 2008,

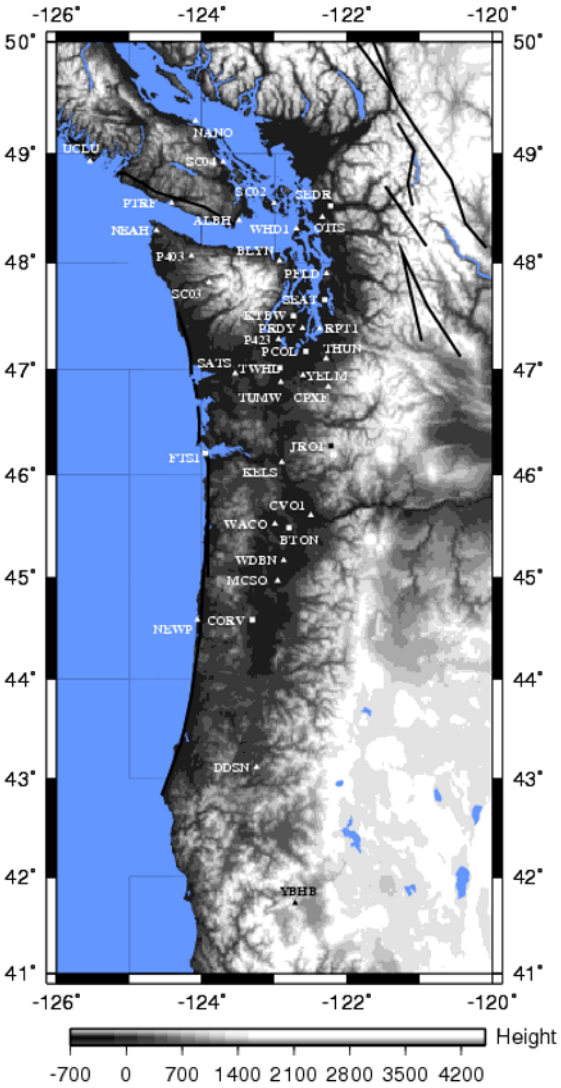

Fig. 2. Geographical location of the selected stations of PANGA along with the approximate situation of some of the active faults in this region.

Zumberge *et al.* 1997). The daily position and covariance matrix of each station is determined in international terrestrial reference frame. Although this method works well enough for determining long-term tectonic rates, it is insufficient for constraining the subtle transients indicative of slow earthquakes. Therefore, to constraint the subtle transient deformation of slow earthquakes using precise point positioning technique, Blewitt presented a new method for resolving the ambiguity of the phase observations in 1996 (Blewitt 1989). In other words, compared to traditional method which uses ionospheric constraints, the above strategy is a method for resolving phase ambiguities in the large base lines, up to 2000 km in length. As such, the method increases the accuracy of the determined coordinates threefold. In the final step, the regional stabilization of the PANGA network is performed by applying a transformation to each daily position. This stabilization means the minimization of the daily and seasonal irregularities in ITRF by removing common errors. This technique is particularly useful where the length of the observation is short and the relative effect of the residual seasonal noise is potentially large. For this purpose, a set of 42 reference stations in the North American plate is used; 23 of them are located in the Pacific Northwest and the remainders are distributed on the stable North American plate interior or in other regional networks in western North America (Miller *et al.* 2001, Wdowinski *et al.* 1997).

Figure 2 illustrates the geographical position of the stations used in this study for detecting the episodic tremors and slips. Here, triangles represent the stations where the occurrences of the slow earthquakes are confirmed through the LS-HE method. Moreover, stations represented by squares are those at which the occurrences of slow slips are not approved by the applied method.

4. DISCUSSION AND CONCLUSION

The episodic tremor and slip as a type of slow earthquakes has the main characteristic of these events, namely, a much longer duration than the other seismic events. This characteristic feature is seen as a low frequency component in the coordinate time series of the GPS stations located in this territory. Therefore, the detection of the corresponding low frequency component is naturally expected to be plausible using an appropriate spectral analysis technique.

Dong *et al.* (2002) analyzed the seasonal variations of the GPS-derived site position time series. The term seasonal variations in that research refer to both annual and semi-annual periods. There are numerous potential contributors to the seasonal variations in site positions, such as thermal expansion, solid earth and ocean tides, *etc*. Some of the seasonal variations

contribute in both the horizontal and vertical coordinates whereas the others, such as the bedrock thermal expansion, primarily contribute to vertical positions. According to Szeliga *et al.* (2008) the cumulative surface transient deformation of the best detected ETSs in Cascadia is about a few millimeters in 8 years. This is far smaller than many of the existing seasonal variations in the GPS time series such as the thermal expansion. Therefore, to detect episodic tremors and slips, the seasonal variations contributing by more than a few millimeters should be removed first from the coordinate time series of each station. However, by removing the seasonal variations, ETSs whose recurrence intervals are close to 12 months (12 months $\pm$ Nyquist frequency) cannot be detected from the detrended time series.

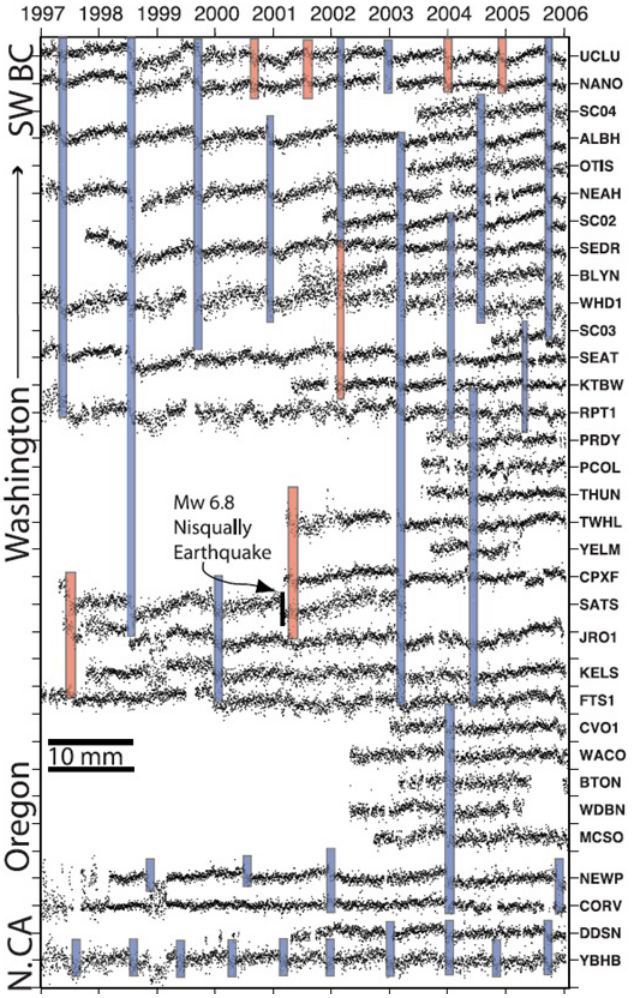

Fig. 3. The detected ETSs in 33 GPS stations of PANGA network by using wavelet transform. Blue boxes indicate slip events either well recorded with GPS or corroborated by observations of subduction zone tremor. Red lines indicate spatially coherent transient GPS deformation typical of slow slip events that uncorroborated at the time by tremor from Szeliga *et al*. (2008). Colour version of this figure is available in electronic edition only.

Szeliga *et al*. (2008) used 33 GPS stations (including those used in this research) as well as the wavelet analysis for detecting the onset time and the mean period of slow slip events. Figure 3 illustrates the outcome for each station. In this figure, the time series of each station is plotted after removing the hardware offsets, seasonal effects, and linear trend. Here, vertical boxes indicate the onset time of tremors and slips computed using wavelet transform.

In the proposed study area, the analysis of seismic data recorded by the seismometers confirms the occurrence of several tremor bursts at or next to the location of these stations. For example, 47 tremors were detected within a month at different parts of Cascadia (Aguiar 2007). Figure 4 highlights the locations of these tremors using a cube grid. As indicated, the star color changes as the day of the month advances, going from blue to green and to red. As seen, one of these tremor bursts is exactly located in the vicinity of the station ALBH.

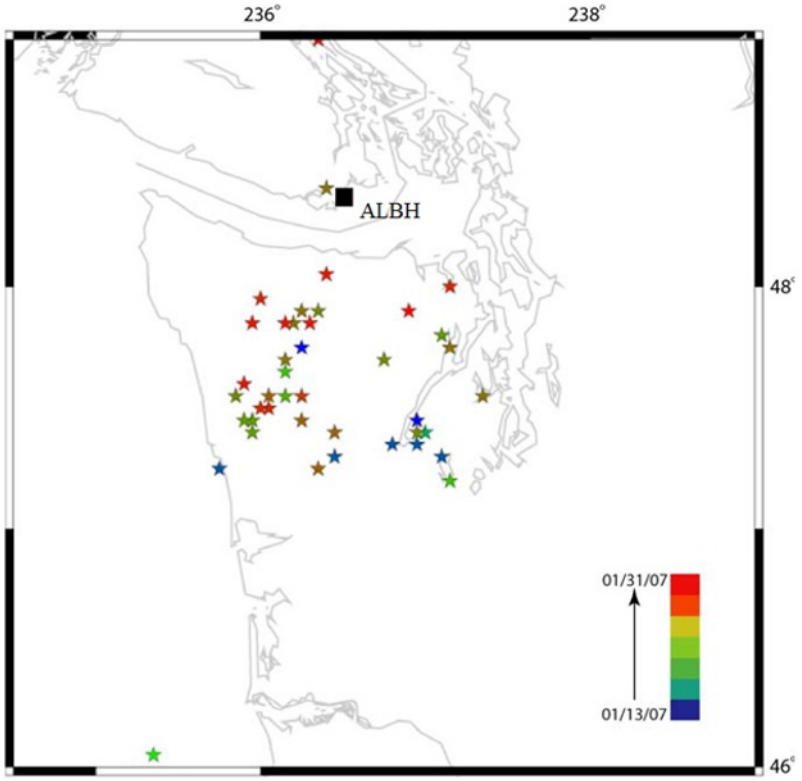

Fig. 4. Surface projection of the locations of tremor bursts from the January 2007 event using a $60 \times 60 \times 21$ cube grid and the position of ALBH from Aguiar (2007). Colour version of this figure is available in electronic edition only.

For the stations that are close to the plate interface and located at the vicinity of a tremor, the residual time series exhibits a sawtooth behavior. This shape distinguishes the episodic nature of these events which is seen in the time series of the east component of the station ALBH given in Figs. 3 and 4. The vertical time series are not used in determining the ETS times especially due to the larger scatter for this component that is common globally (Holtkamp and Brudzinski 2010). Moreover, the sawtooth behavior of the ETS events is more obvious in the time series of the east component as compared to the north component.

As discussed before, the current paper has used the LS-HE method for detecting the episodic tremors. Consequently, at first, the long-term (seasonal effects) and linear trends are removed from the coordinate time series of each given station. In case a receiver antenna is changed, the resulting offsets are modeled using Heaviside functions and are eliminated from observations. Using the method outlined in Section 2, the existing frequencies in the coordinate time series are then estimated separately for each station. Figure 5 illustrates the time series of station ALBH as one of the points in the study area. Figure 5a, b demonstrates the raw time series of this station and the same after removing linear, semiannual, and annual effects.

The spectrum of the residual time series has been then constructed using the frequencies identified by the LS-HE method. As such, the frequency with maximum power spectrum (the one having the greatest contribution to signal construction) is the main periodic constituent (predominant frequency) following the semiannual and annual ones. Figure 6 illustrates the power spec-

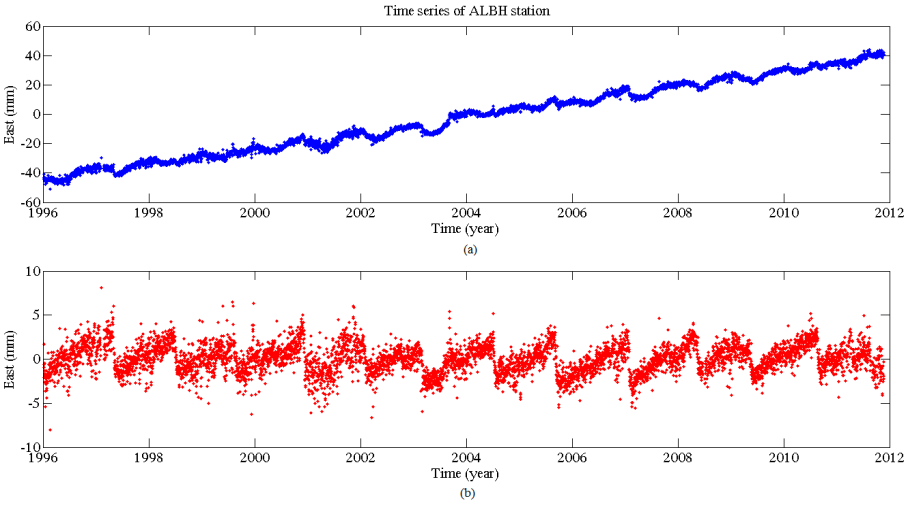

Fig. 5. Time series of station ALBH: (a) raw time series, and (b) residual time series.

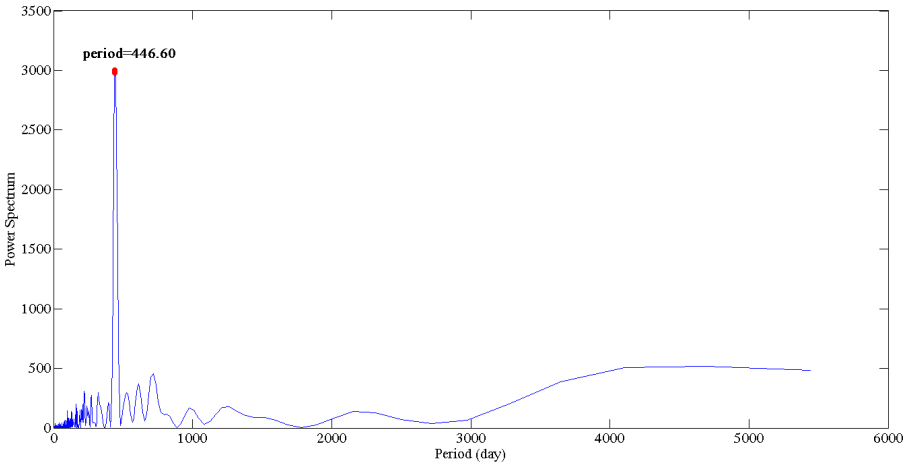

Fig. 6. The power spectrum of station ALBH.

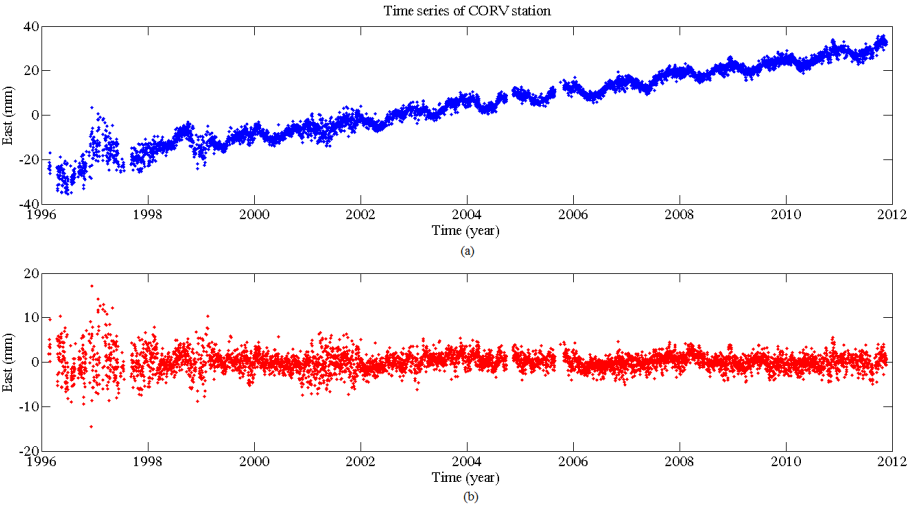

Fig. 7. Time series of station CORV: (a) raw time series, and (b) residual time series.

trum of the residual time series for ALBH where the maximum power spectrum corresponds to the frequency of 446.60 days.

Table 1 shows the position of the GPS stations used in this research together with the main periodic constituent identified through the above procedure. The adopted confidence level is 99%. In this table, rows printed in bold are the GPS stations at which the detected predominant frequencies are not confirmed by the other reports. As Fig. 2 indicates, squares are used for distinguishing these stations from the others.

Table 1

The detected period of the events in the evaluated stations by LS-HE method

No.	Name of station	Geographical latitude (in degrees)	Geographical longitude (in degrees)	The detected period of events (in days)
1	ALBH	48.39	236.51	446.60
2	BLYN	48.02	237.07	491.53
3	**BTON**	**45.48**	**237.20**	**1669.94**
4	**CORV**	**44.58**	**236.69**	**1627.76**
5	CPXF	46.84	237.74	1160.39
6	CVO1	45.61	237.50	682.02
7	DDSN	43.12	236.75	613.61
8	**FTS1**	**46.20**	**236.04**	**3708.82**
9	**JRO1**	**46.27**	**237.78**	**3023.00**
10	KELS	46.12	237.10	563.85
11	**KTBW**	**47.50**	**237.25**	**196.28**
12	MCSO	44.97	237.04	673.78
13	NANO	49.29	235.91	382.88
14	NEAH	48.29	235.37	440.45
15	NEWP	44.59	235.94	690.40
16	OTIS	48.42	237.66	1007.23
17	**PCOL**	**47.17**	**237.43**	**1943.70**
18	PFLD	47.89	237.72	425.98
19	PRDY	47.39	237.39	1142.70
20	PTRF	48.54	235.586	224.77
21	P403	48.06	235.85	436.01
22	P423	47.28	237.06	1134.50
23	RPT1	47.39	237.62	491.97
24	SATS	46.96	236.46	662.72
25	**SEAT**	**47.65**	**237.69**	**2836.15**
26	**SEDR**	**48.52**	**237.77**	**3180.52**
27	SC02	48.55	236.99	447.80
28	SC03	47.81	236.10	451.61
29	SC04	48.92	236.29	447.99
30	THUN	47.11	237.71	335.75
31	TUMW	46.98	237.08	840.08
32	**TWHL**	**47.02**	**237.08**	**3105.73**
33	UCLU	48.92	234.45	380.96
34	WACO	45.52	237.01	693.30
35	WDBN	45.17	237.13	682.58
36	WHD1	48.31	237.30	469.29
37	YBHB	41.73	237.29	332.69
38	YELM	46.95	237.39	334.79

Based on previous studies (*e.g*., Miller *et al.* 2002, Szeliga *et al*. 2008), the period of these events depends on the rheology and geophysical characteristics of the study area. The occurrence period for the episodic slips in this region varies from 9.5 to 14 months. Moreover, several slips with periods ranging 1.5 and 3 years are also reported for the geographical latitudes range of 46° N to 48° N. In these regions, LS-HE suggests a period which is comparable with the mean period already reported for this area.

For the stations that are far away from the plate interface and the surface projection of the tremors locations, such as CORV, the characteristic sawtooth shape disappears from the residual time series. Figure 7 illustrates the residual time series of station CORV at latitude 44.5°, far from the location of these earthquakes. A comparison of the residual time series of ALBH and CORV shows how the sawtooth behavior disappears with their distance from the surface projection of the tremors locations. As Fig. 3 shows, the sequential tremor events in CORV do not occur regularly. According to Szeliga *et al.* (2004), the absence of a sawtooth shape in the residual time series of this station is consistent with relatively narrow, offshore locked and transition zones at this latitude, also suggested from vertical deformation rates (Julian 2002).

The obtained results (see Table 1) show that the period of the first detected component with maximum amplitude in plot of the power spectrum of all stations, except SEAT, SEDR, BTON, CORV, FTS1, JRO1, TWHL, PCOL and KTBW, is equivalent to the reported periods for slow earthquakes at the corresponding positions of these stations.

Reported results for station SEAT, using wavelet transform, also illustrate an irregular behavior for episodic tremors at this station (see Fig. 3). This can be realized by a comparison of the duration of sequential tremor bursts detected using the GPS time series of this station. For example, no tremor is seen between two sequential tremor bursts at this station in the years 1998 and 2002; however, the time interval between the first two reported events there, is less than 2 years. This is also valid for TWHL, JRO1, FTS1, and SEDR stations whose further details can be seen in Fig. 3.

With regard KTBW, since the length of available data is quite short (2010 to 2011) the LS-HE method cannot suggest any harmonic for ETS in the coordinate time series of this point. Also, the coordinate time series in stations BTON and PCOL starts from 2003. Since the proposed LS-HE method is sensitive to the length of data (Mousavian and Hossainali 2012); the acquired results for the above stations are unreliable. At the same time, as Fig. 3 shows, since only one tremor could be recorded at these stations by 2006, it is hard to suggest the occurrence of slow slips with episodic character there.

Acknowledgments. We are indebted to the Pacific Northwest Geodetic Array (PANGA) for giving us an access to the GPS time series data during the course of this research.

References

Aguiar, A.C. (2007), Seismic constraints on slow slip events within the Cascadia subduction zone, M.Sc. Thesis, Central Washington University, Washington, USA.

Amiri-Simkooei, A.R. (2007), Least-squares variance component estimation: Theory and GPS applications, Ph.D. Thesis, Delft University of Technology, Publication on Geodesy, Vol. 64, Netherlands Geodetic Commission, Delft.

Amiri-Simkooei, A.R., and J. Asgari (2012), Harmonic analysis of total electron contents time series: methodology and results, *GPS Solut*. **16**, 1, 77-88, DOI: 10.1007/s10291-011-0208-x.

Amiri-Simkooei, A.R., and C.C.J.M. Tiberius (2007), Assessing receiver noise using GPS short baseline time series, *GPS Solut.* **11**, 1, 21-35, DOI: 10.1007/s10291-006-0026-8.

Amiri-Simkooei, A.R., C.C.J.M. Tiberius, and P.J.G. Teunissen (2007), Assessment of noise in GPS coordinate time series: methodology and results, *J. Geophys. Res.* **112**, B7, 1978-2012, DOI: 10.1029/2006JB004913.

Atwater, B.F. (1987), Evidence for great Holocene earthquakes along the outer coast of Washington State, *Science* **236**, 4804, 942-944, DOI: 10.1126/science.236.4804.942.

Beroza, G.C., and S. Ide (2011), Slow earthquakes and nonvolcanic tremor, *Ann. Rev. Earth Planet. Sci.* **39**, 271-296, DOI: 10.1146/annurev-earth-040809-152531.

Blewitt, G. (1989), Carrier phase ambiguity resolution for the Global Positioning System applied to geodetic baselines up to 2000 km, *J. Geophys. Res*. **94**, B8, 10187-10203, DOI: 10.1029/JB094iB08p10187.

Dong, D., P. Fang, Y. Bock, M.K. Cheng, and S. Miyazaki (2002), Anatomy of apparent seasonal variations from GPS-derived site position time series, *J. Geophys. Res*. **107**, B4, ETG-9.1-ETG-9.16, DOI: 10.1029/2001JB000573.

Holtkamp, S., and M.R. Brudzinski (2010), Determination of slow slip episodes and strain accumulation along the Cascadia margin, *J. Geophys. Res*. **115**, B4, B00A17, DOI: 10.1029/2008JB006058.

Ito, Y., and K. Obara (2006), Dynamic deformation of the accretionary prism excites very low frequency earthquakes, *Geophys. Res. Lett.* **33**, 2, L02311, DOI: 10.1029/2005GL025270.

Ito, Y., K. Obara, K. Shiomi, S. Sekine, and H. Hirose (2007), Slow earthquakes coincident with episodic tremors and slow slip events, *Science* **315**, 5811, 503-506, DOI: 10.1126/science.1134454.

Julian, B. (2002), Seismological detection of slab metamorphism, *Science* **296**, 5573, 1625-1626, DOI: 10.1126/science.1072602.

Kao, H., and S.-J. Shan (2004), The source-scanning algorithm: mapping the distribution of seismic sources in time and space, *Geophys. J. Int*. **157**, 2, 589-594, DOI: 10.1111/j.1365-246X.2004.02276.x.

Kao, H., S.-J. Shan, H. Dragert, G. Rogers, J.F. Cassidy, and K. Ramachandran (2005), A wide depth distribution of seismic tremors along the northern Cascadia margin, *Nature* **436**, 7052, 841-844, DOI: 10.1038/ nature03903.

Kao, H., P.J. Thompson, G. Rogers, H. Dragert, and G. Spence (2007), Automatic detection and characterization of seismic tremors in northern Cascadia, *Geophys. Res. Lett*. **34**, 16, L16313, DOI: 10.1029/2007GL030822.

Kao, H., P.J. Thompson, S.-J. Shan, G. Rogers, and H. Dragert (2008), Tremor Activity Monitoring in northern Cascadia, *Eos Trans. AGU* **89**, 42, 405-406, DOI: 10.1029/ 2008EO420001.

Kao, H., S.-J. Shan, H. Dragert, and G. Rogers (2009), Northern Cascadia episodic tremor and slip: A decade of tremor observations from 1997 to 2007, *J. Geophys. Res.* **114**, B11, B00A12, DOI: 10.1029/2008JB006046.

Linde, A.T., M.T. Gladwin, M.J.S. Johnston, R.L. Gwyther, and R.G. Bilham (1996), A slow earthquake sequence on the San Andreas fault, *Nature* **383**, 6595, 65-68, DOI: 10.1038/383065a0.

Miller, M.M., D.J. Johnson, C.M. Rubin, H. Dragert, K. Wang, A. Qamar, and C. Goldfinger (2001), GPS-determination of along-strike variation in Cascadia margin kinematics: Implications for relative plate motion, subduction zone coupling, and permanent deformation, *Tectonics* **20**, 2, 161-176, DOI: 10.1029/2000TC001224.

Miller, M.M., T.I. Melbourne, D.J. Johnson, and W.Q. Sumner (2002), Periodic slow earthquakes from the Cascadia subduction zone, *Science* **295**, 5564, 2423, DOI: 10.1126/science.1071193.

Mousavian, R., and M.M. Hossainali (2012), Detection of main tidal frequencies using least squares harmonic estimation method, *J. Geodetic Sci*. **2**, 3, 224-233, DOI: 10.2478/v10156-011-0043-6.

Obara, K. (2002), Nonvolcanic deep tremor associated with subduction in southwest Japan, *Science* **296**, 5573, 1679-1681, DOI: 10.1126/science.1070378.

Obara, K., K. Kasahara, S. Hori, and Y. Okada (2005), A densely distributed high-sensitivity seismograph network in Japan: Hi-net by National Research Institute for Earth Science and Disaster Prevention, *Rev. Sci. Instrum*. **76**, 2, 021301-021301-12, DOI: 10.1063/1.1854197.

Rogers, G., and H. Dragert (2003), Episodic tremor and slip on the Cascadia subduction zone: The chatter of silent slip, *Science* **300**, 5627, 1942-1943, DOI: 10.1126/science.1084783.

Satake, K., K Shimazaki, Y. Tsuji, and K. Ueda (1996), Time and size of a giant earthquake in Cascadia inferred from Japanese tsunami records of January 1700, *Nature* **379**, 6562, 246-249, DOI: 10.1038/379246a0.

Szeliga, W., T.I. Melbourne, M.M. Miller, and V.M. Santillan (2004), Southern Cascadia episodic slow earthquakes, *Geophys. Res. Lett.* **31**, 16, L16602, DOI: 10.1029/2004GL020824.

Szeliga, W., T. Melbourne, M. Santillan, and M. Miller (2008), GPS constraints on 34 slow slip events within the Cascadia subduction zone, 1997-2005, *J. Geophys. Res*. **113**, B4, B04404, DOI: 10.1029/2007JB004948.

Teunissen, P.J.G. (2000), *Adjustment Theory: An Introduction*, Series on Mathematical Geodesy and Positioning, Delft University Press, Delft, 193 pp.

Teunissen, P.J.G., D.G. Simons, and C.C.J.M. Tiberius (2005), Probability and observation theory, Delft University of Technology, Faculty of Aerospace Engineering, Lecture notes AE2-E01.

Thompson, J. (2011), *Cascadia's Fault: The Coming Earthquake and Tsunami That Could Devastate North America*, Counterpoint Press, Berkeley.

Vaníček, P. (1969), Approximate spectral analysis by least-squares fit, *Astrophys. Space Sci*. **4**, 4, 387-391, DOI: 10.1007/BF00651344.

Wdowinski, S., Y. Bock, J. Zhang, P. Fang, and J. Genrich (1997), Southern California permanent GPS geodetic array: Spatial filtering of daily positions for estimating coseismic and postseismic displacements induced by the 1992 Landers earthquake, *J. Geophys. Res.* **102**, B8, 18057-18070, DOI: 10.1029/97JB01378.

Zumberge, J.F., M.B. Heflin, D.C. Jefferson, M.M. Watkins, and F.H. Webb (1997), Precise point positioning for the efficient and robust analysis of GPS data from large networks, *J. Geophys. Res*. **102**, B3, 5005-5017, DOI: 10.1029/96JB03860.

Received 9 December 2012
Received in revised form 8 May 2013
Accepted 14 May 2013